Varied signature splitting phenomena in odd proton nuclei

Yang Sun,[1,2] Da Hsuan Feng,[1,2] and Shuxian Wen[3]
[1] *Department of Physics and Atmospheric Science, Drexel University, Philadelphia, Pennsylvania 19104*
[2] *Physics Division, Oak Ridge National Laboratory, Oak Ridge, Tennessee 37831*
[3] *China Institute of Atomic Energy, P.O. Box 275, Beijing, People's Republic of China*
(Received 20 April 1994)

Varied signature splitting phenomena in odd proton rare-earth nuclei are investigated. Signature splitting as functions of K and j in the angular momentum projection theory is explicitly shown and compared with those of the particle rotor model. The observed deviations from these rules are due to the band mixings. The recently measured ^{169}Ta high spin data are taken as a typical example where fruitful information about signature effects can be extracted. Six bands, two of which have not yet been observed, were calculated and discussed in detail in this paper. The experimentally unknown band head energies are given.

PACS number(s): 21.10.Re, 21.60.Ev, 27.70.+q

Although there were many discussions in the past about signature splitting [1–4], they were mainly devoted to odd neutron rare-earth nuclei. One reason for this could be because for such nuclei, bands are built up by nearly pure $i_{\frac{13}{2}}$ intruders. Therefore, their structures are simple. For the odd proton nuclei, however, the proton Fermi level is surrounded by more j subshells, all of which have rather different characters and interact with each other, thus complicating the structure. It is also for this reason that we believe that additional information about signature splitting could arise from such nuclei. On the other hand, modern detectors and techniques allow one not only to analyze high spin data in the yrast band but also more sidebands. That different bands within one nucleus show distinguished behaviors is certainly a challenge and a crucial test of the existing nuclear theories. The recently reported measurement [5] of the odd proton rare-earth nucleus, ^{169}Ta, which has provided us with fruitful information for our understanding of signature splitting, is an excellent example for such a purpose.

Signature [6] is a quantum number specifically appearing in a deformed intrinsic system. It is neither a universal quantum number nor a concept in the conventional spherical shell model. It is related to the invariance of a system with quadrupole deformation under a rotation of 180° around a principal axis (e.g., the x axis)

$$\hat{R}_x = e^{i\pi \hat{J}_x}. \tag{1}$$

If the system is axially symmetric, only the rotation around any principal axes other than the symmetry one can define the signature quantum number. Thus, signature is a consequence of a deformed system and corresponds to a "deformation invariance" with respect to space and time reflection [7]. For the even-even nuclei the signature operator $\hat{R}_x$ has two eigenvalues ± 1, while in the odd mass nuclei $\pm i$. By requiring that the deformed core be filled up from the bottom in the twofold degenergate orbits with nucleons having signature $\pm i$, the total signature of the ground-state band for the even-even nucleus is $+1$. For an odd mass nucleus, depending on its total spin, it can assume two different values. In fact, it is customary to assign

$$\alpha_I = \tfrac{1}{2}(-1)^{I-1/2} \tag{2}$$

as the signature quantum number for a state of spin I of an odd mass nucleus. Such a rotational band with a sequence of levels differing in spin by $1\hbar$ is now divided into two branches, each consisting of levels differing in spin by $2\hbar$ and classified by the signature quantum number $\alpha_I = \pm\frac{1}{2}$, respectively. Experimentally, one often observes an energy splitting for the two branches.

The origin of such an energy splitting in a rotational band can be understood in the particle-rotor model. For the strong coupling limit, the symmetrized wave function [6] can be written as

$$|\,\phi^{IM}_{iK}\rangle = \sqrt{\frac{2I+1}{16\pi^2}}\left\{D^I_{MK}(\Omega)\,|\,iK\rangle + (-)^{I-K}D^I_{M-K}(\Omega)\,|\,\overline{iK}\rangle\right\}, \tag{3}$$

where $D^I_{MK}(\Omega)$ is the irreducible representation of the rotational group, Ω the orientation of the rotor, and $|\,\overline{iK}\rangle$ the time-reversed state of the particle state $|\,iK\rangle$. The wave function of Eq. (3) has the factor $(-1)^{I-K}$ in its second term. Taking the Coriolis coupling into account by the first order perturbation theory, this I-dependent factor will appear in the energy spectrum and contribute only to the $K=\frac{1}{2}$ band

$$E_{i,K=\frac{1}{2}} \sim \left\{I(I+1) - a_i(-1)^{I-\frac{1}{2}}(I+\tfrac{1}{2})\right\}, \tag{4}$$

where a_i is the so-called decoupling parameter [6] and depends on the j components which contribute to the particle state $|\,iK=\frac{1}{2}\rangle$. From the spectrum of Eq. (4), one sees that for a positive (negative) decoupling parameter, the levels with even (odd) values of $I-\frac{1}{2}$ [$I=\frac{1}{2},\frac{5}{2},\frac{9}{2},\ldots$ ($I=\frac{3}{2},\frac{7}{2},\frac{11}{2},\ldots$)] are shifted downward, thus splitting

one band into two branches. The splitting amplitude and phase are, respectively, determined by the size and the sign of a_i. This decoupling effect can explain the rather distorted bands for $K = \frac{1}{2}$ in many odd mass nuclei within the context of the particle-rotor model.

Of course, the splitting is not necessarily confined to the $K = \frac{1}{2}$ case. It appears in the $K = \frac{1}{2}$ band in the particle-rotor model because the Coriolis interaction couples bands which differ in K quantum number by ± 1 (the $\Delta K = 1$ selection rule) and the Coriolis matrix has its diagonal elements only between the $K = \frac{1}{2}$ state and its time reversed state in the first order perturbation theory. However, as an observable phenomenon, splitting of one band into two branches should also manifest itself in any nuclear many-body theory. To conform to the standard nomenclature, in this paper we shall keep using the name "signature splitting." In fact, it was shown [8] that similar symmetrized wave functions also exsit in the angular momentum projection theory [9,10]. Although, in the projection theory, there is no explicit decoupling parameter, the phenomenon of signature splitting clearly shows up when an intrinsic single particle state is projected onto states of good angular momentum. One of the distinguished features of the angular momentum projection theory is that the signature splitting can in fact persist up to the $K = \frac{5}{2}$ band [11,12], well beyond the $K = \frac{1}{2}$ band. This is obviously important to explain the data.

The angular momentum projection theory established in the late 1970's [9,10] has been proven to be a powerful model to quantitatively account for many high spin phenomena [8,12,13]. Very recently, using this model, we have successfully explained the anomalous crossing frequency in odd proton rare-earth nuclei [14]. Since the model has already been discussed in detail elsewhere [10,12,13], we shall only outline the major points of the theory which are relevant to the present discussions.

The ansatz for the angular momentum projected wave function is given by

$$|IM\rangle = \sum_{\kappa} f_{\kappa} \hat{P}^{I}_{MK_{\kappa}} |\varphi_{\kappa}\rangle, \tag{5}$$

where κ labels the basis states. Acting on an intrinsic state $|\varphi_{\kappa}\rangle$, the projection operator $\hat{P}^{I}_{MK}$ [15] generates states of good angular momentum, thus restoring the necessary rotational symmetry which was violated in the deformed mean field. In this paper we assume that the intrinsic states have axial symmetry. Thus, the basis states $|\varphi_{\kappa}\rangle$ must have K as a good quantum number. For an odd proton system, the basis is spanned by the set

$$\left\{ \alpha^{\dagger}_{p_l}|\phi\rangle,\ \alpha^{\dagger}_{n_i}\alpha^{\dagger}_{n_j}\alpha^{\dagger}_{p_l}|\phi\rangle \right\}. \tag{6}$$

The quasiparticle vacuum is $|\phi\rangle$ and $\{\alpha_m, \alpha^{\dagger}_m\}$ are the quasiparticle annihilation and creation operators for this vacuum; the index n_i (p_i) runs over selected neutron (proton) quasiparticle states and κ in Eq. (5) runs over the configurations of Eq. (6). The vacuum $|\phi\rangle$ is obtained by diagonalizing a deformed Nilsson Hamiltonian [16] followed by a BCS calculation. In the calculation we have used three major shells, i.e., N=4, 5, and 6 (N=3, 4, and 5) for neutrons (protons) as the configuration space. The BCS blocking effect associated with the last unpaired proton is approximately taken into account by allowing all the odd number of protons to participate without blocking any individual level. Thus the vacuum in this case is an average over the two neighboring even-even nuclei. The size of the basis states is determined by using energy windows of 1.5 MeV and 3 MeV for the 1- and 3-qp states, respectively. Consequently, about 50 low-lying configurations are constructed.

In this paper, we have used the following Hamiltonian [10]

$$\hat{H} = \hat{H}_0 - \frac{1}{2}\chi \sum_{\mu} \hat{Q}^{\dagger}_{\mu}\hat{Q}_{\mu} - G_M \hat{P}^{\dagger}\hat{P} - G_Q \sum_{\mu} \hat{P}^{\dagger}_{\mu}\hat{P}_{\mu}, \tag{7}$$

where $\hat{H}_0$ is the spherical single-particle shell model Hamiltonian. The second term is the quadrupole-quadrupole interaction and the last two terms are the monopole and quadrupole pairing interactions, respectively. The interaction strengths are determined as follows: the quadrupole interaction strength χ is adjusted so that the known quadrupole deformation ϵ_2 from the Hartree-Fock-Bogoliubov self-consistent procedure [17] is obtained. For example, for ^{169}Ta it is 0.225; the monopole pairing strength G_M is adjusted to the known energy gap

$$G_M = \left[20.12 \mp 13.13 \frac{N-Z}{A} \right] \cdot A^{-1}, \tag{8}$$

where the minus (plus) sign is for neutrons (protons). The quadrupole pairing strength G_Q is assumed to be proportional to G_M and the proportional constant is fixed to be 0.20 for all the bands calculated in the present work.

The weights f_{κ} in Eq. (5) are determined by diagonalizing the Hamiltonian $\hat{H}$ in the basis given by of Eq. (6). This will lead to the eigenvalue equation (for a given spin I)

$$\sum_{\kappa'} (H_{\kappa\kappa'} - E N_{\kappa\kappa'}) f_{\kappa'} = 0, \tag{9}$$

with the Hamiltonian and norm overlaps given by

$$\begin{aligned} H_{\kappa\kappa'} &= \langle \varphi_{\kappa}|\hat{H}\hat{P}^{I}_{K_{\kappa}K'_{\kappa'}}|\varphi_{\kappa'}\rangle, \\ N_{\kappa\kappa'} &= \langle \varphi_{\kappa}|\hat{P}^{I}_{K_{\kappa}K'_{\kappa'}}|\varphi_{\kappa'}\rangle. \end{aligned} \tag{10}$$

The energies of each band are given by the diagonal elements of Eq. (10)

$$E_{\kappa}(I) = \frac{\langle \varphi_{\kappa}|\hat{H}\hat{P}^{I}_{KK}|\varphi_{\kappa}\rangle}{\langle \varphi_{\kappa}|\hat{P}^{I}_{KK}|\varphi_{\kappa}\rangle} = \frac{H_{\kappa\kappa}}{N_{\kappa\kappa}}. \tag{11}$$

A diagram in which $E_{\kappa}(I)$ of various bands are plotted against the spin I will be referred to [13] as a band diagram. Although the results obtained from diagonalizing the Hamiltonian of Eq. (7) can be compared with the data, global behaviors of the bands can already be understood by these diagonal elements, as we shall see below.

We begin by showing the varied signature splittings of the one-quasiproton bands [Eq. (11)] in Fig. 1, where we have plotted the energy differences $E_I - E_{I-1}$ as a function of angular momentum I. These bands are taken from the present ^{169}Ta calculation, thus reflecting the realistic situations of the one-quasiproton bands in the rare-earth region. In Fig. 1(a), which takes the K bands of the $1h_{\frac{11}{2}}$ j subshell as examples, we show how the splitting amplitude decreases with K and increases with I. It is clearly seen that the signature splitting is not restricted just to the $K = \frac{1}{2}$ case. In fact, we see that the splitting is large even for $K = \frac{5}{2}$ where a clear zigzag at higher spins is observed. Beyond $K \geq \frac{7}{2}$, the splitting is sufficiently diminished.

Unlike Fig. 1(a), in Fig. 1(b) we have plotted six $K = \frac{1}{2}$ bands from different j subshells. These bands are from $N = 4$ and 5 proton major shells, with some being close to the proton Fermi level and thus are experimentally observed. Here the general feature is that the splitting amplitude increases with increasing j and the bands from neighboring j have opposite splitting phases. This is consistent with the particle rotor model [see Eq. (4)]. What is particularly interesting is the $2d_{\frac{3}{2}}$ case ($\frac{1}{2}^+[411]$ band). For this band, the lower corners of the curve due to the splitting are nearly zero, which implies a zero $\Delta I = 1$ transition energies. This implies also that one should expect that there will be an interesting energy degeneracy in the neighboring levels for this band, as we will see below.

The band diagrams for ^{169}Ta are plotted in Fig. 2. Although there are about 50 bands in the calculations, only several lowest-lying ones are plotted to illustrate the

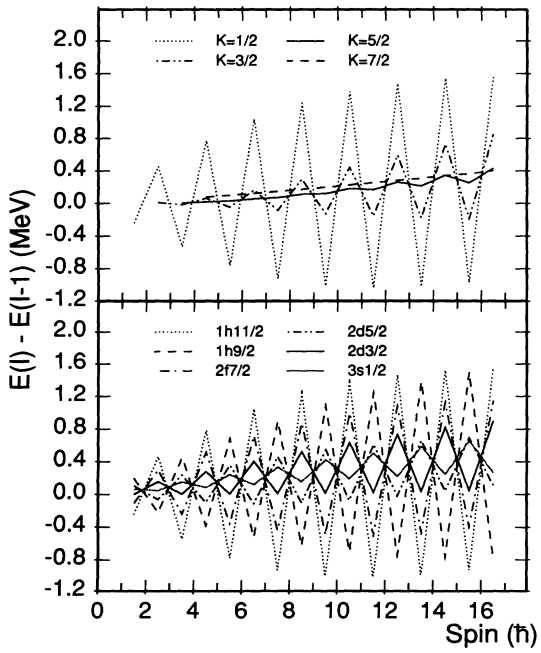

FIG. 1. Signature splitting as function of spin. Bands are characterized by different curve types as shown in the figure boxes. (a) Top: different K bands of the $1h_{\frac{11}{2}}$ subshell. (b) Bottom: $K = \frac{1}{2}$ bands from different j subshells.

physics. It is expected that for ^{169}Ta, the states $\frac{1}{2}^-[541]$, $\frac{7}{2}^-[523]$, $\frac{9}{2}^-[514]$, $\frac{1}{2}^+[411]$, $\frac{5}{2}^+[402]$, and $\frac{7}{2}^+[404]$ are close to the proton Fermi level and thus bands based on these configurations are likely to be observed. In Fig. 2, each plotted band has a definite K quantum number. However, we stress that K will not be conserved due to the band mixing. In fact, it is only an approximately conserved quantity, depending on how strongly these bands are mixed by the diagonalization. This is especially true for bands lying close in energy and with the same symmetry. From Fig. 2 we will expect that at relatively low spins, K is approximately a good quantum number because bands are separately distributed in this spin region. As the nucleus rotates more rapidly, level density in a given energy interval will be higher [13] and the admixing of K will be enhanced. The amount of mixing can easily be analyzed from the wave functions. Through the mixing, the bands near the yrast line can display some of the properties of the higher-lying bands. In fact, the observed phenomenon signature inversion in the odd-odd rare-earth nuclei was explained by the mechanism of band mixing [8].

In Fig. 2(a), we see that the $\frac{9}{2}^-[514]$ band rises smoothly with a steeper slope (smaller moment of inertia). It crosses the 3-qp band at a lower spin ($\frac{31}{2}\hbar$), which is consistent with the data [5]. Since this is a high-K band, one would not expect signature splitting to occur. However, there is another band $\frac{5}{2}^-[532]$ and its corresponding 3-qp band. The splitting for this band is weak but distinct and will admix with the $\frac{9}{2}^-[514]$ band. On the other hand, mixing of the $\frac{1}{2}^-[541]$ band with its neighboring bands is negligibly small because the former is originated from different j subshells. Consequently, the experimentally observed small splittings [5] in the $\frac{9}{2}^-[514]$ band are clearly caused by the mixing with $\frac{5}{2}^-[532]$ band and therefore show the splitting phase of this band.

A rather different behavior is seen from the $\frac{1}{2}^-[541]$ band: Due to a strong decoupling effect, it is splitted into two branches and are separated from each other by about 1 MeV. Experimentally, the unfavored high-lying bands are very weakly populated and therefore, in most cases, only the favored branch with signature $\alpha = \frac{1}{2}$ has been observed [5]. This is the common observation for the $\frac{1}{2}^-[541]$ band in the rare-earth region. As we have mentioned before, the zigzag amplitude increases with spin. This effect, as can be clearly seen in Fig. 2(a), brings the $\frac{5}{2}\hbar$ level to be lower in energy than that of spin $\frac{1}{2}\hbar$, thus explaining why the observed bandhead of $\frac{1}{2}^-[541]$ is usually $\frac{5}{2}\hbar$ and not $\frac{1}{2}\hbar$. Furthermore, the band crossing of the $\frac{1}{2}^-[541]$ with its 3-qp band occurs at spin $\frac{37}{2}\hbar$, which again reproduces the data [5]. The $\frac{7}{2}^-[523]$ band, which lies somewhat higher in energy than the $\frac{1}{2}^-[541]$ favored branch, has not been observed experimentally.

There are two types of interesting energy degeneracies in the positive parity bands as shown in Fig. 2(b). First, the two bands $\frac{5}{2}^+[402]$ and $\frac{7}{2}^+[404]$ are found to be nearly degenerate for the entire band, thus making

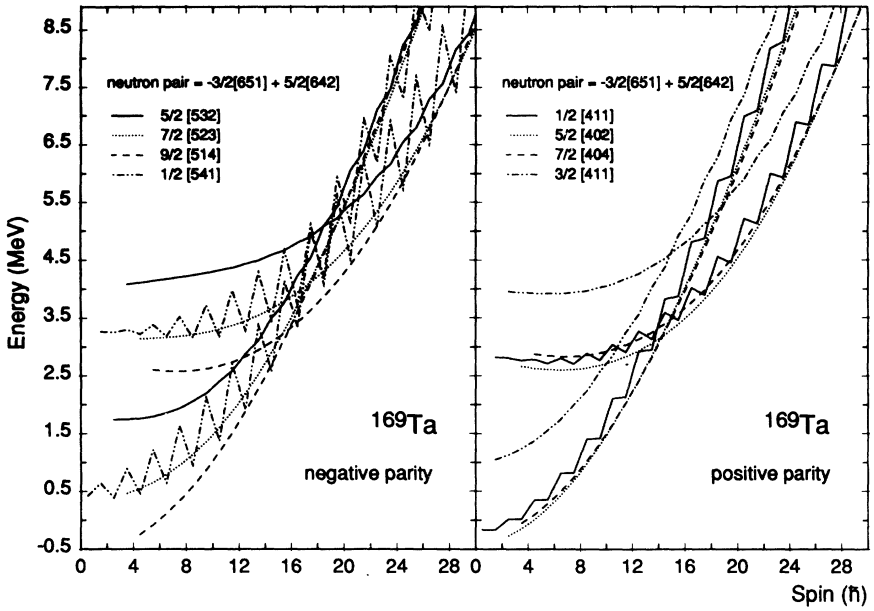

FIG. 2. Band diagram for several lowest lying one-quasiproton and the corresponding 3-qp (one-quasiproton + neutron pair) bands in ^{169}Ta. Bands are characterized by different curve types as shown in the figure boxes. Note that each 1-qp band shares the same curve type with its corresponding 3-qp band, but they can be easily distinguished due to their energy separations (The bandhead of 1-qp is typically lower than that of the corresponding 3-qp by 2.5 MeV.) Note also that the slope of a curve $\omega = \frac{dE}{dI}$ is the rotational frequency and its inverted value measures the moment of inertia of the band. (a) Left: negative parity bands. (b) Right: positive parity bands.

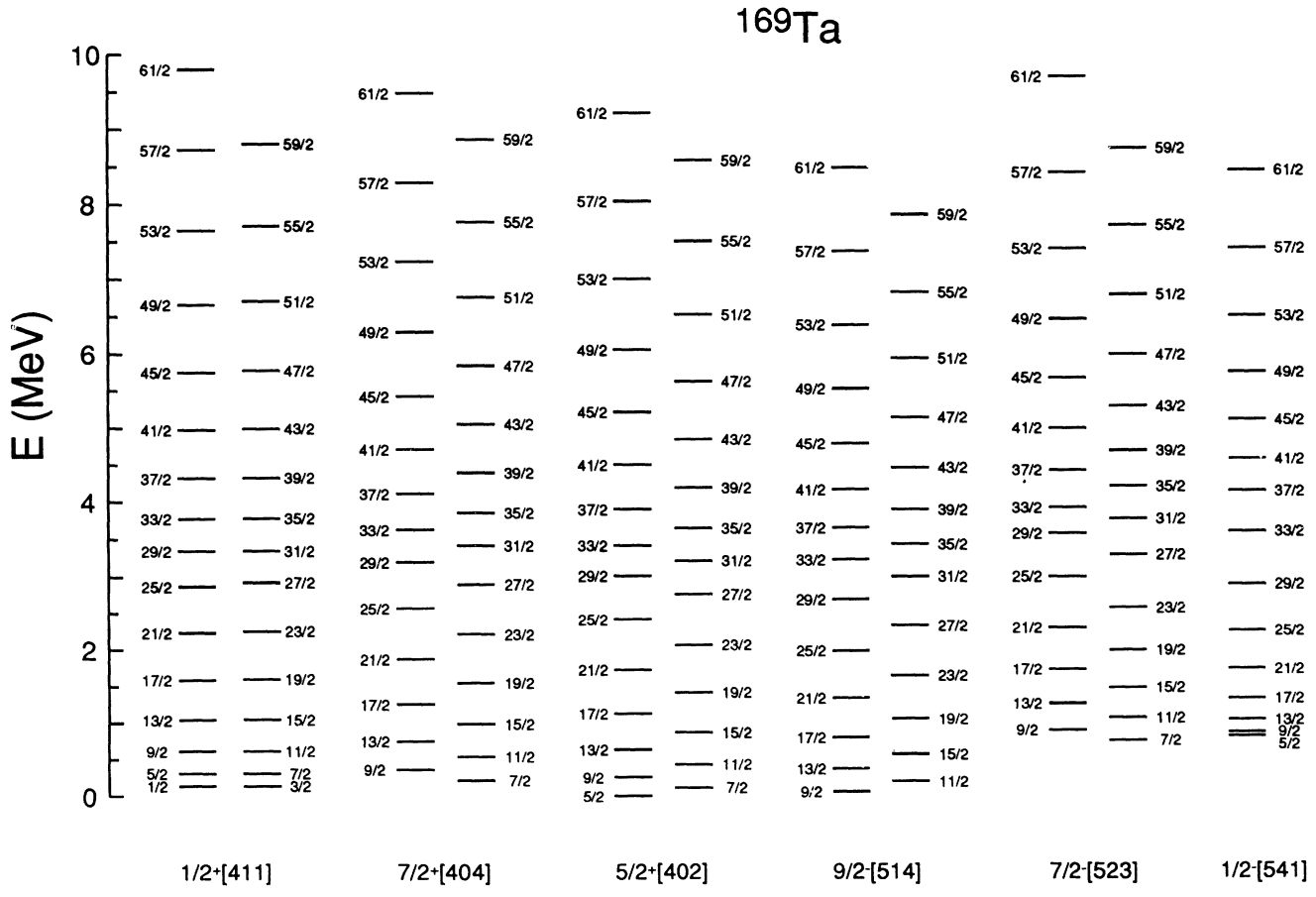

FIG. 3. Theoretical level scheme of ^{169}Ta.

the experimental separation near impossible. Although their interaction causes a slight repulsion, they nevertheless remain parallel and have nearly identical moments of inertia. This will be shown clearly later on in Fig. 3. In this situation, it is very difficult to distinguish them experimentally since they have the same transition energies along their decay sequences. In fact, only one of them was analyzed from the data and was assigned as

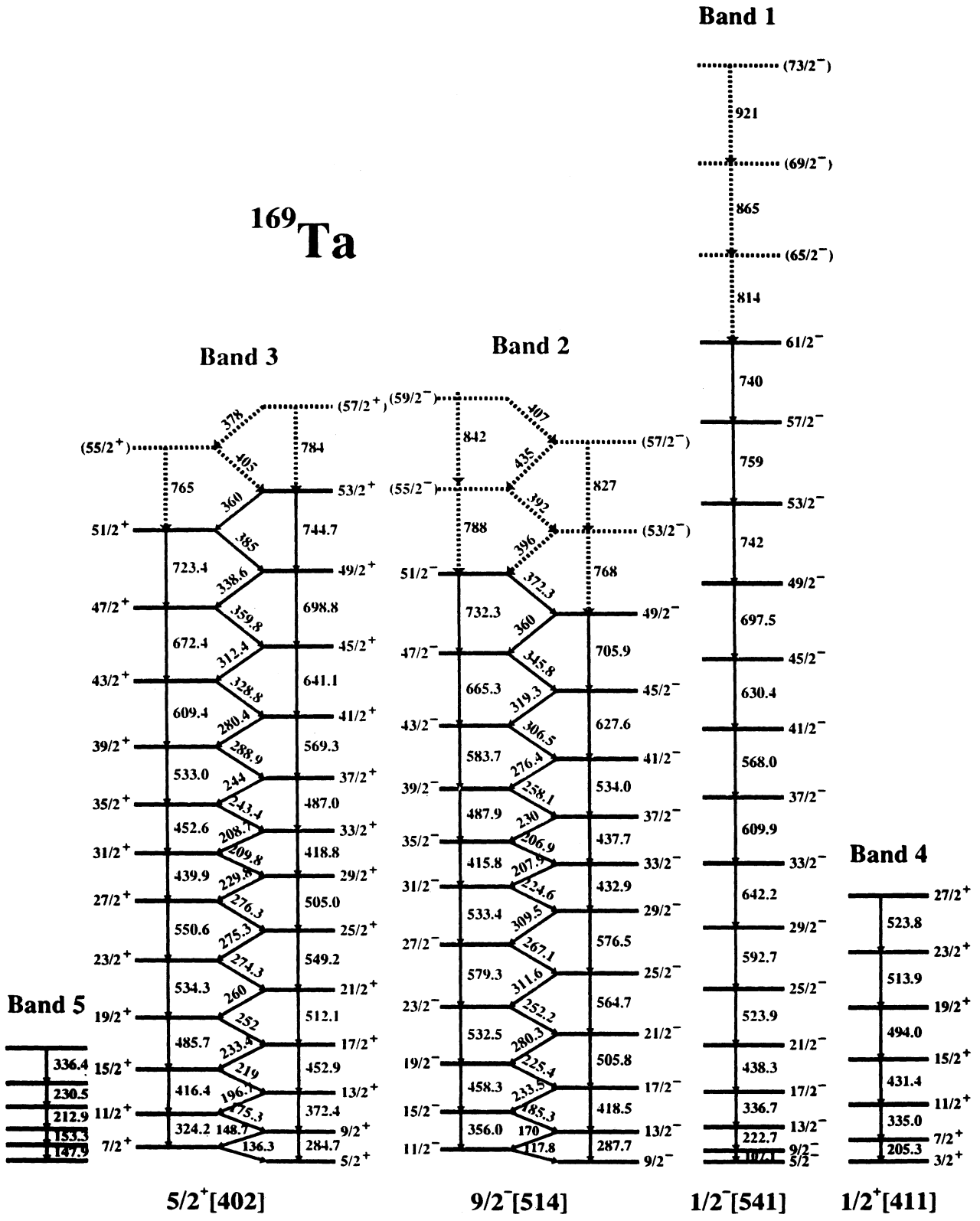

FIG. 4. Experimental level scheme of ^{169}Ta. This is the same as the Fig. 2 of Ref. [5].

$\frac{5}{2}^+[402]$ [5]. Thus, our calculation clarifies as to why the most likely observed $\frac{7}{2}^+[404]$ band in fact has escaped notice in the analysis of the data. Clearly, this degeneracy is determined by the special locations of the two bands and thus should be isotope dependent. It would be interesting to know which one is favored in energy along the isotopic and the isotonic chains.

Second, as was pointed out in Fig. 1(b), the signature splitting in the special configuration $\frac{1}{2}^+[411]$ in ^{169}Ta resulted in an accidental degeneracy between the two signature partners. Such a degeneracy implies that the $\Delta I = 2$ transition energies along the two signature branches are identical. The reason why only one signature branch in the $\frac{1}{2}^+[411]$ band is observed [5] is not due to the large signature splitting as in the $\frac{1}{2}^-[541]$ case, but by the accidental degeneracy. If this were true, then the $\Delta I = 1$ transition energy between the two branches (e.g., $\frac{5}{2}^+ \rightarrow \frac{3}{2}^+$) should also be identical to the $\Delta I = 2$ transition along the same branch (e.g., $\frac{7}{2}^+ \rightarrow \frac{3}{2}^+$). We anticipate that one could ascertain these predictions by experimentally distinguishing the $M1$ and the $E2$ transitions along the $\frac{1}{2}^+[411]$ decay sequences. It should be noted that in other odd proton rare-earth nuclei, such accidental degeneracy may not occur because the splitting is determined by the decoupling effect which can be different from case to case.

All three positive parity bands ($\frac{1}{2}^+[411]$, $\frac{5}{2}^+[402]$, and $\frac{7}{2}^+[404]$) cross their respective 3-qp bands roughly at spin $\frac{29}{2}\hbar$. The crossings change their configurations from 1-qp to 3-qp. Indeed, the $\frac{1}{2}^+[411]$ band suddenly encounters a highly mixing region at spin $\frac{29}{2}\hbar$. This may be why the measured band terminates at spin $\frac{27}{2}\hbar$ [5]. The experimentally observed small splitting in the $\frac{5}{2}^+[402]$ band at high spins [5], from our analysis, is due to the mixing with the $\frac{3}{2}^+[411]$ band which shows distinct zigzag in its 3-qp configuration.

Finally, the entire calculated level scheme for ^{169}Ta is presented in Fig. 3. This scheme should be compared to the experimental scheme given in Fig. 2 of Ref. [5]. For completeness, the same diagram is given as Fig. 4 of this paper. In Fig. 3 three lowest-lying positive and negative parity bands are shown (see Fig. 2 of this paper for their exact locations before band mixing). Two of them ($\frac{7}{2}^+[404]$ and $\frac{7}{2}^-[523]$) are our predictions. Because of the missing linking transitions, the excitation energies of the bandheads cannot be determined experimentally. Our calculation suggests that the $I = \frac{5}{2}$ of the band $\frac{5}{2}^+[402]$ is the lowest and is therefore set to be the reference level in Fig. 3. The excitation energies of the other bandheads related to the reference level are 142 keV ($I = \frac{1}{2}$ in $\frac{1}{2}^+[411]$ band), 215 keV ($I = \frac{7}{2}$ in $\frac{7}{2}^+[404]$ band), 52 keV ($I = \frac{9}{2}$ in $\frac{9}{2}^-[514]$ band), 755 keV ($I = \frac{7}{2}$ in $\frac{7}{2}^-[523]$ band), and 807 keV ($I = \frac{5}{2}$ in $\frac{1}{2}^-[541]$ band). The $\frac{9}{2}^-[514]$ band has the lowest state at each spin and is therefore the yrast band. The nearly degenerate two signature branches of the band $\frac{1}{2}^+[411]$ is clearly seen. The two bands $\frac{5}{2}^+[402]$ and $\frac{7}{2}^+[404]$ [see Fig. 2(b)], due to their interactions, are now shifted from each other in a parallel manner by roughly 200 keV. Yet, they maintain identical transition energies. The two predicted bands $\frac{7}{2}^+[404]$ and $\frac{7}{2}^-[523]$ could be candidates for the experimentally observed but not yet assigned band 5 in Ref. [5]. We should point out that at very high spins (around $\frac{53}{2}\hbar$), one expects that the 5-qp states will cross the 3-qp states, thus lowering the energy levels after the crossing. Since such 5-qp configurations have not been included in the present calculations, some of the computed high spin levels are found to be too high in energy.

In conclusion, we have investigated the signature splitting phenomena in the framework of the angular momentum projection theory. The dependences of the splitting on the 3-component of the total angular momentum K and on the particle angular momentum j are explicitly given. We have demonstrated that in the projection theory, the signature splitting can persist beyond the $K = \frac{1}{2}$ band and is also a diagonal effect for high-K bands. These features are clearly different from the particle rotor model. Furthermore, band mixing brings the behaviors of higher-lying bands into the near yrast bands, resulting in some observed deviations from the signature splitting rules.

The ^{169}Ta data are taken as an example to test our theory. Fruitful information about signature splitting can be extracted from this nucleus. We have pointed out that different explanations as to why only one signature branch is observed may work for the two $K = \frac{1}{2}$ bands: namely, the accidental degeneracy of the two branches in the $\frac{1}{2}^+[411]$ and the usual large signature splitting in the $\frac{1}{2}^-[541]$ band. Another degeneracy which resulted in the identical transition energies after band mixing, are found in $\frac{5}{2}^+[402]$ and $\frac{7}{2}^+[404]$ bands. Finally, the entire calculated level scheme with six bands are given. We also suggest the bandhead excitations. Although the even-even nuclei have recently been investigated in detail [18], this paper is the first application of the angular momentum projection theory to the side bands in the odd-A system.

Useful discussions with Mike Guidry and Lee L. Riedinger are acknowledged. Yang Sun is most grateful to the College of Arts and Science of Drexel University for the provision of a fellowship. This work was partially supported by the United States National Science Foundation. Oak Ridge National Laboratory is managed by Martin Marietta Energy Systems, Inc., for the U.S. Department of Energy under Contract No. DEAC05-84OR21400.

[1] J. Kownacki *et al.*, Nucl. Phys. **A394**, 269 (1983).
[2] S. Shastry *et al.*, Nucl. Phys. **A470**, 253 (1987).
[3] L.L. Riedinger *et al.*, Prog. Part. Nucl. Phys. **28**, 75 (1992).
[4] W.F. Mueller *et al.*, Phys. Rev. C **50**, 1901 (1994).
[5] S.G. Li *et al.*, Nucl. Phys. **A555**, 435 (1993).
[6] A. Bohr and B.R. Mottelson, *Nuclear Structure* (Benjamin, New York, 1975), Vol. II.
[7] A. Bohr, Rev. Mod. Phys. **48**, 365 (1976).
[8] K. Hara and Y. Sun, Nucl. Phys. **A531**, 221 (1991).
[9] K. Hara and S. Iwasaki, Nucl. Phys. **A332**, 61 (1979).
[10] K. Hara and S. Iwasaki, Nucl. Phys. **A348**, 200 (1980).
[11] K. Hara and S. Iwasaki, Nucl. Phys. **A430**, 175 (1984).
[12] K. Hara and Y. Sun, Nucl. Phys. **A537**, 77 (1992).
[13] K. Hara and Y. Sun, Nucl. Phys. **A529**, 445 (1991).
[14] Y. Sun, S. Wen, and D.H. Feng, Phys. Rev. Lett. **72**, 3483 (1994).
[15] P. Ring and P. Schuck, *The Nuclear Many Body Problem* (Springer Verlag, New York, 1980).
[16] C.G. Andersson *et al.*, Nucl. Phys. **A309**, 41 (1978).
[17] I.L. Lamm, Nucl. Phys. **A125**, 504 (1969).
[18] Y. Sun and J.L. Egido, Phys. Rev. C **50**, 1893 (1994).